

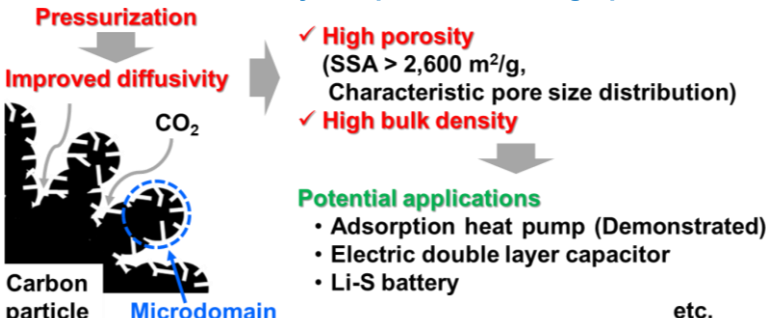
Accounts of Materials & Surface Research

Pressurized physical activation method for production of high-performance activated carbons based on microdomain pore structure model

Jin Miyawaki*

*Institute for Materials Chemistry and Engineering, Kyushu University
6-1 Kasuga-koen, Kasuga, Fukuoka 816-8580, Japan
miyawaki@cm.kyushu-u.ac.jp*

Growing demand for high-performance porous carbon materials stimulates developments of new preparation and modification technologies. Activated carbon (AC), one of representative porous carbon materials, is also desired to improve the physicochemical properties, especially the porosity, for upgrading the application characteristics and exploiting the new application fields. To produce AC, activation is a key process, because it governs the porosity. In this article, a simple production method of AC with a highly developed pore structure is introduced. An idea of the “pressurized physical activation” was come up with an understanding of physical and chemical activation mechanisms based on a recognition of microdomain, which is a basic structure unit of artificial carbon materials. This pressurized physical activation method gave AC with a specific surface area larger than 2600 m²/g, which is difficult to achieve by a conventional atmospheric pressure physical activation. Although chemical activation method can produce AC with higher degree of pore development in high activation yield, the pressurized physical activation is considered as an option to provide a high degree of pore development at a relatively low-cost way. Together with the high porosity, the pressurized physical AC showed a characteristic pore size distribution and a high bulk density. Taking these advantages, a superior potential of the pressurized physical AC was demonstrated as a relatively-inexpensive and high-performance adsorbent in adsorption heat pump system using ethanol as a refrigerant. Traditional AC still has huge rooms to boost its performance and broaden its field of application. New idea for facile production and modification methods of AC with purpose-designed porosity and surface property is eagerly anticipated.



✓ **High porosity**
(SSA > 2,600 m²/g,
Characteristic pore size distribution)

✓ **High bulk density**

Potential applications

- Adsorption heat pump (Demonstrated)
- Electric double layer capacitor
- Li-S battery

etc.

Keyword: Activated carbon, Microdomain, Pore, Pressurized physical activation

Jin Miyawaki received his Dr. Sci. in 2001 from Chiba University under the supervision of Prof. Katsumi Kaneko. He started his academic career in 2001 as a postdoctoral fellow of The Energy Institute at The Pennsylvania State University, USA, in a research project conducted by Prof. Ljubisa R. Radovic. Then, he studied as a postdoctoral fellow from 2003 to 2008 in a Solution-Oriented Research for Science and Technology program of The Japan Science and Technology (JST-SORST) organized by Prof. Sumio Iijima. In 2008, he moved to Institute for Materials Chemistry and Engineering, Kyushu University as an assistant professor, and promoted to an associate professor in 2013. His research interests include arbitrary controls of porosity and surface functionality of porous carbon materials together with developments of porosity assessment technology.



Pressurized physical activation method for production of high-performance activated carbons based on microdomain pore structure model

Jin Miyawaki*

Institute for Materials Chemistry and Engineering, Kyushu University

6-1 Kasuga-koen, Kasuga, Fukuoka 816-8580, Japan

miyawaki@cm.kyushu-u.ac.jp

1. Prolusion

Porous carbon materials as represented by activated carbon (AC) are widely used in various application fields, such as gas purification/separation/storage, water-treatment, solvent recovery, catalyst support, and electric double layer capacitor. The high performance and multifunctionality of the porous carbon materials stand on the highly developed pore structure with the huge specific surface area (SSA). To further extend the performance and exploit new application areas of porous carbon materials, therefore, the increase of degree of pore development based on a precise understanding of pore structure is indispensable.

Through observations using scanning electron microscope (SEM) and scanning tunneling microscope (STM), we have

confirmed that most of artificial carbon materials including various ACs consisted of a basic structure unit named “microdomain”.^{1)–4)} On the basis of the recognition that the artificial carbon materials are an aggregate of microdomains, a new pore structure model of AC has been proposed as shown in **Figure 1**.²⁾

Based on this microdomain pore structure model, in this article, differences in the pore development mechanisms between physical and chemical activation processes for AC preparation are firstly discussed from a structural point of view.⁴⁾ The understanding of mechanism of physical activation suggested an idea of a novel pressurized physical activation method: The effectiveness of pressurization in physical activation is then demonstrated as a simple production method

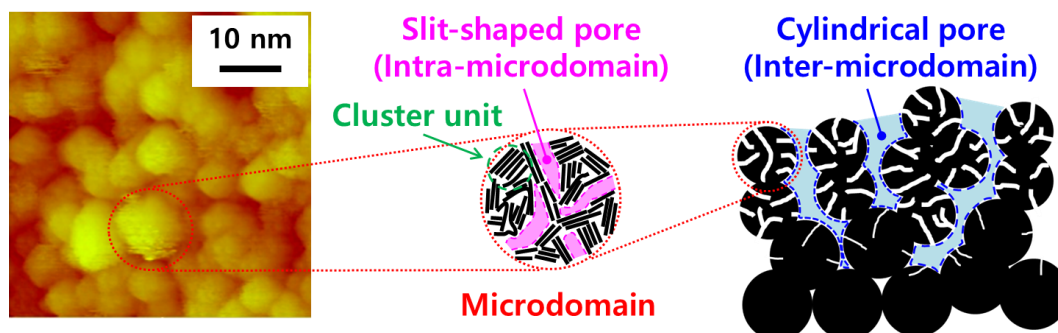


Figure 1. (Left) Scanning tunneling microscope image of activated carbon fiber and (center and right) new pore structure model of activated carbons based on recognition of microdomains.

of AC with a highly developed pore structure.⁵⁾ Finally, an applicability of pressurized physical AC as an adsorbent in adsorption heat pump (AHP) is introduced.⁶⁾

2. Structural elucidation of physical and chemical activation mechanisms based on microdomain structure model⁴⁾

Activation is a process to develop pore structure in carbonized substances derived from various raw materials, and is classified into physical and chemical methods. A lower AC production cost is an advantage of physical activation, while chemical activation can provide AC with highly developed pore structure in high yield. Although many researches have been carried out to elucidate reasons of higher degree of pore development for chemical AC,^{7)–9)} differences in the pore development mechanisms between physical and chemical activation processes have not been well clarified, especially from a structural point of view. In this study, therefore, an elucidation of the differences in the structural mechanisms of these two activation processes was carried out, based on the microdomain pore structure model.

As a starting material, a spherical carbon (C6) prepared by the carbonization of a spherical phenol resin (BEAPS series, ASAHI YUKIZAI CORPORATION, Japan) at 600°C for 1 h in N₂ was used. Relatively uniform particle size and shape of C6 allowed to discuss influences of the activation process on size and shape of carbon particles. For physical and chemical activations, steam and potassium hydroxide (KOH) were used as activating agents, respectively. The prepared steam- and KOH-ACs were abbreviated as

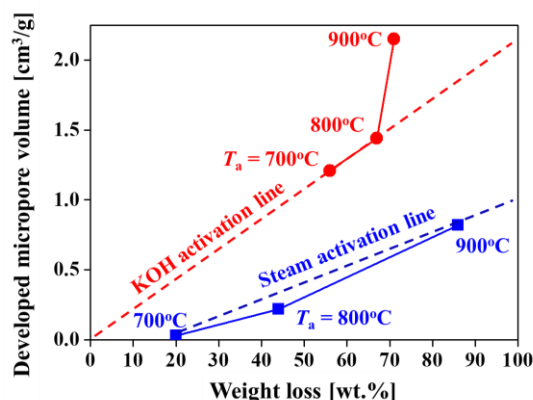


Figure 2. Relationship between weight loss and developed micropore volume of (blue square) steam- and (red circle) KOH-activated carbons prepared at different activation temperatures, T_a .⁴⁾ (Reprinted from Carbon, 114, 98–105. Copyright (2017), with permission from Elsevier.)

C6S_x and C6K_x, respectively, where x indicates the number of the first digit of the activation temperature, T_a : e.g. C6S8 was obtained by steam activation at $T_a = 800^\circ\text{C}$.

Figure 2 shows the relationship between weight loss (= 100 – activation yield [wt.%]) and developed micropore volume from C6 by activation. Lower degree of pore development of steam-AC was apparently observed as compared to KOH-AC. In detail, at $T_a = 700^\circ\text{C}$, KOH activation induced a large weight loss than steam activation. On the other hand, much larger increase of micropore volume was found for C6K7 (1.21 cm³/g), whereas C6S7 showed a negligible increment (0.03 cm³/g). This indicates that the weight loss of about 20 wt.% by steam activation at $T_a = 700^\circ\text{C}$ was mainly due to a gasification of solid carbon without micropore development, whilst KOH activation at the same activation temperature gave rise to an effective pore development. At a higher activation temperature, degree of pore development increased by both steam and

KOH activations. However, the increasing ratio of micropore volume against weight loss was more apparent for KOH-AC than for steam-AC. When KOH activation was carried out at $T_a = 900^\circ\text{C}$, the micropore volume increased sharply without noticeable weight loss (4 wt.% reduction). This is likely due to different pore development mechanism, namely potassium intercalation mechanism, as previously reported.^{7), 10)}

SEM and STM observations revealed that spherical shapes of carbon particles and microdomains of C6 were nearly unchanged by both steam and KOH activations. However, a distinct difference was found in size depending on the activation method. **Figure 3** summarizes changes of mean sizes of carbon particles and microdomains by two activation methods depending on T_a . Even at high T_a , and thus, at high degree of pore development, both particle and microdomain sizes of KOH-AC remained almost the same with those of the pristine C6. In contrast, steam-AC showed significant decreases in both particle and microdomain sizes with an increase of T_a .

Based on the above-mentioned findings, a schematic model of the structural mechanism of pore development during physical and chemical activation is proposed, as shown in **Figure 4**. The STM observation showed that each particle of C6 was an aggregate of a large number of nanometer-size spherical microdomains. By KOH activation at $T_a = 700^\circ\text{C}$, almost no size changes of particles and microdomains were induced. This indicates that, for C6K7, pores developed in the intra-microdomain region, giving rise to a largely increased micropore volume. On the other hand, steam activation at low

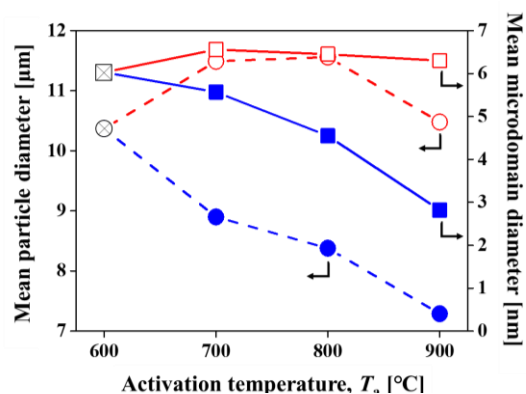


Figure 3. Change of mean sizes of (circle) particles and (square) microdomains by steam and KOH activations depending on activation temperature, T_a . The solid (blue) and open (red) symbols denote steam- and KOH-activated carbons, respectively.⁴⁾ (Reprinted from Carbon, 114, 98–105. Copyright (2017), with permission from Elsevier.)

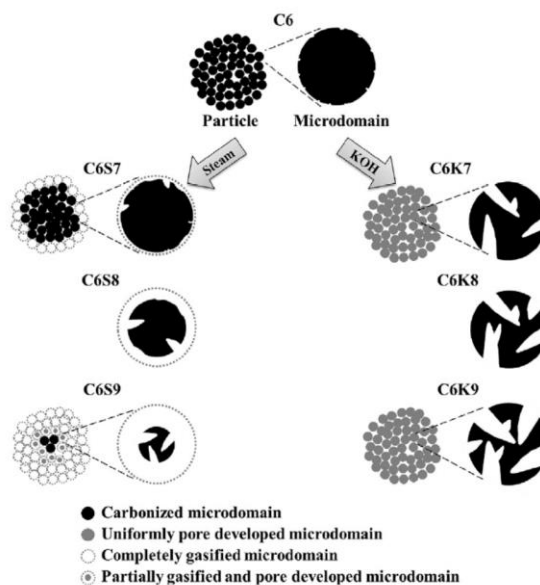


Figure 4. Structural mechanism model of pore development for steam- and KOH-activated carbons.⁴⁾ (Reprinted from Carbon, 114, 98–105. Copyright (2017), with permission from Elsevier.)

temperature of 700°C did not induce the pore development, regardless of the weight loss of about 20 wt.% and apparent decreases of particle and microdomain sizes. This suggests that the oxidative reaction of steam

progressed preferentially at the external surface of the carbon particles and microdomains, resulting in a gasification of the outer parts. An increase of T_a gave the micropore development also for steam-AC, although the pore developing efficiency was less than that for KOH-As. At $T_a = 900^\circ\text{C}$, a widening of pore size was occurred by the intercalation mechanism for KOH-AC. In the case of steam-AC, however, the preferential gasification of microdomains located at the periphery of carbon particles progressed together with the pore development in the microdomains, giving rise to the large weight loss and remarkable size-reductions of particle and microdomains of C6S9.

In summary, KOH activation (chemical activation) induces a uniform pore development overall for all microdomains comprising carbon particles; however, in the case of steam activation (physical activation), pores are developed in remaining microdomains after the inhomogeneous gasification from the outer surface of carbon particles and their microdomains. The different pore development mechanisms of physical and chemical activations cause differences in the degree of pore development and the activation yield.

3. Pressurized physical activation: A simple production method for activated carbon with a highly developed pore structure⁵⁾

As discussed in Section 2, lower activation yield and limited pore development of physically activated carbons are due to inhomogeneous gasification from the outer surface of carbon particles and microdomains. On the hypothesis that insufficient diffusivity

of activating agent (activating gas molecule) into core parts of carbon particles and their microdomains causes the inhomogeneous reaction, in other words, conventional physical activation at atmospheric pressure is diffusion-limited reaction, we tried to pressurize the activation gas for improving the diffusivity, and thus, for leading more uniform activation reaction. Previously, we have reported that pressurization improved diffusivity of oxygen gas in pitch fibers, giving rise to the homogeneous stabilization effect.¹¹⁾ In this study, therefore, the effectiveness of pressurization in physical activation was investigated to propose a simple production method for AC with a highly developed pore structure.

The same starting material of spherical carbon (C6) was used in the same way as the previous section. C6 was physically activated at 700–900°C using pure CO₂ as an activation gas at an absolute pressure of 0.1 or 1.0 MPa for the desired time. The obtained ACs were designated as PXTymZ, where X, Y, and Z are the activation pressure [MPa], temperature [°C], and holding time at 900°C [min], if any, respectively: e.g. P0.1T900m5 is AC prepared at 0.1 MPa and 900°C with 5-min holding.

Figure 5 shows a relationship between activation yield and SSA of ACs prepared by conventional atmospheric pressure and pressurized physical activations using CO₂ as activating gas. Here, the ordinate is SSA per weight of AC. A difference between atmospheric pressure physical activation (0.1 MPa) and pressurized physical activation (1.0 MPa) was apparently observed: At a similar yield, the pressurized physical AC (pressurized-AC) showed higher SSA than

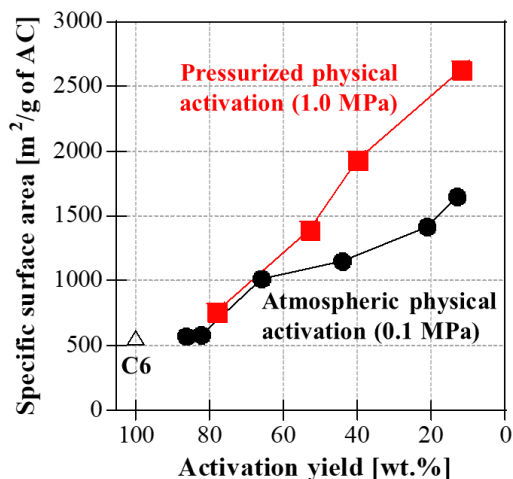


Figure 5. Relationship of activation yield to specific surface area on activated carbon weight basis for activated carbons prepared by (black circle) atmospheric pressure and (red square) pressurized physical activation methods with CO₂ as an activating agent. The result of the starting carbonized material (C6; open triangle) is shown for comparison.¹²⁾

the atmospheric pressure physical AC (atmospheric-AC), indicating the effectiveness of pressurization for pore development. Of note, pressurized physical activation afforded to obtain AC with SSA of 2630 m²/g; such high value is difficult to achieve by conventional atmospheric pressure physical activation.

To discuss how effectively the gasification of solid carbon surely contributes to the pore development, changes of SSA on a starting material (char: C6) weight basis depending on activation yield are shown in **Figure 6**. The char-weight-basis SSA values of pressurized-AC increased up to 40 wt.% of activation yield, whilst those of atmospheric-AC started to decrease above 60 wt.% of activation yield. This indicates that pressurization can suppress the unwanted gasification of solid carbon, giving rise to more efficient pore development as compared with conventional

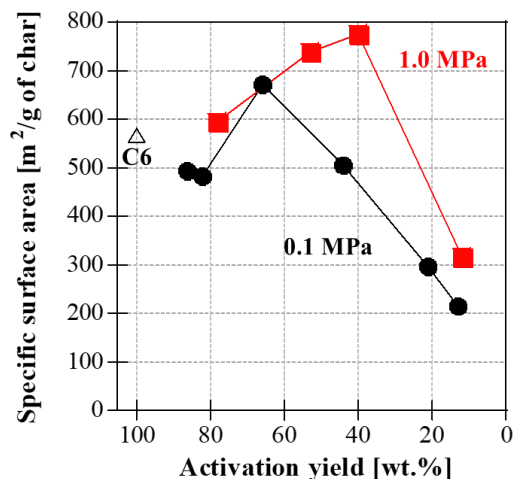


Figure 6. Relationship of activation yield to specific surface area on char weight basis for activated carbons prepared by (black circle) atmospheric and (red square) pressurized physical activation methods with CO₂ as an activating agent. The result of the starting carbonized material (C6; open triangle) is shown for comparison.¹²⁾

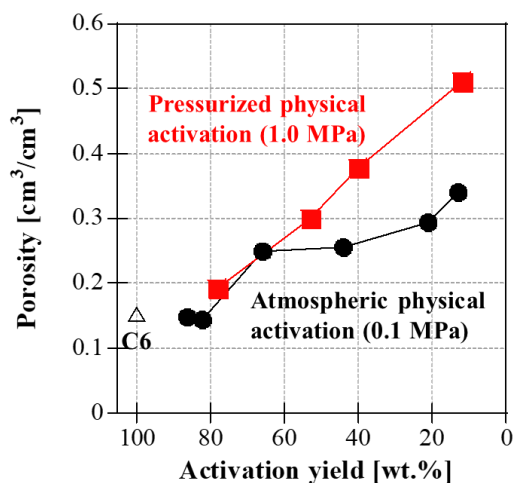


Figure 7. Relationships of activation yield to porosity for activated carbons prepared by (black circle) atmospheric pressure and (red square) pressurized physical activation methods. The result of the starting carbonized material (C6; open triangle) is shown for comparison.¹²⁾

atmospheric pressure physical activation.

Effectiveness of pressurization on pore development was confirmed also from

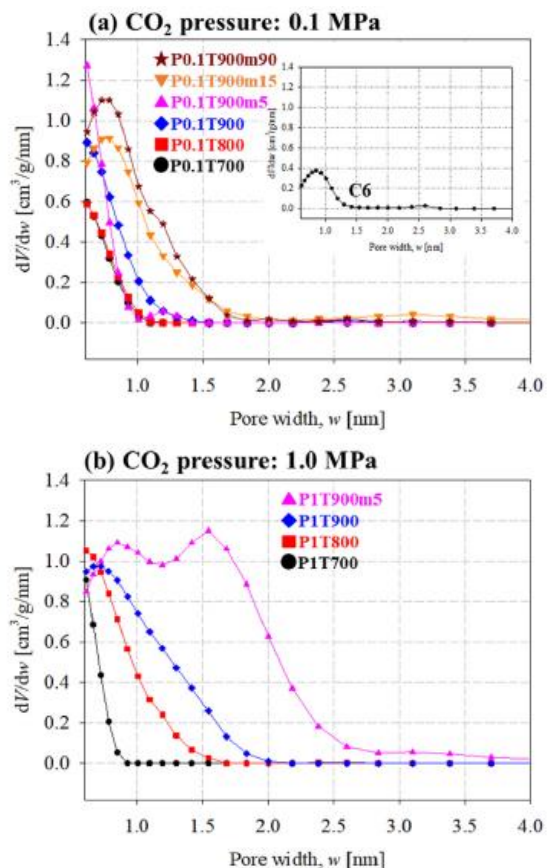


Figure 8. Pore size distributions of (a) atmospheric pressure and (b) pressurized physically activated carbons. (Black circle) P0.1T700 or P1T700; (red square) P0.1T800 or P1T800; (blue rhombus) P0.1T900 or P1T900; (pink triangle) P0.1T900m5 or P1T900m5; (orange inverted triangle) P0.1T900m15; and (brown star) P0.1T900m90. Inset in (a): The results of the starting carbonized material (C6) are shown for comparison.⁵⁾ (Reprinted from Carbon, 183, 735–742. Copyright (2021), with permission from Elsevier.)

porosity as shown in **Figure 7**. From the porosity values of AC with about 12–13 wt.% of activation yield, approximately one third of vessel volume was considered to correspond to the developed pores for atmospheric-AC, whereas almost half of vessel volume was attributed to the developed pores for pressurized-AC.

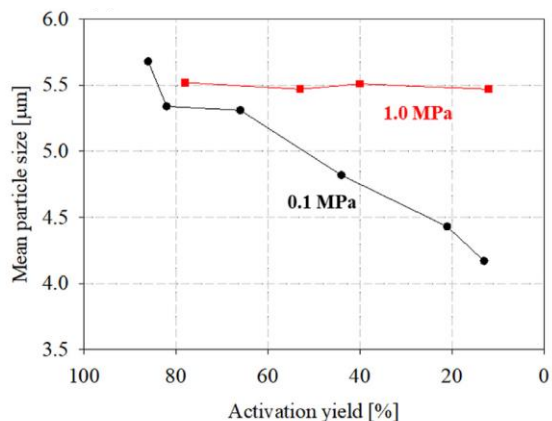


Figure 9. Relationships between mean particle size and activation yield for (black circle) atmospheric pressure and (red square) pressurized physical activations.⁵⁾ (Reprinted from Carbon, 183, 735–742. Copyright (2021), with permission from Elsevier.)

Pressurization provided not only a remarkable increase of degree of pore development, but also a characteristic pore size distribution (**Figure 8**). Conventional atmospheric pressure physical activation using CO₂ as an activating gas predominantly developed narrow micropores less than 1.0 nm of pore width. In contrast, CO₂ activation at 1.0 MPa gave the development of wider micropores; especially, P1T900m5 showed a characteristic pore size distribution with a peak pore width of about 1.6 nm.

Figure 9 shows relationships between activation yield and mean particle size estimated from SEM images for atmospheric- and pressurized-ACs. Although mean particle size of atmospheric-AC decreased with decrease in activation yield, no change was found for pressurized-AC, indicating that pressurization allowed the uniform pore development, at least at the particle level. On the other hand, STM observation revealed that mean microdomain sizes of P1T900m5 and P0.1T900m90, which showed similar activation yields, were 5.0 and 6.1 nm,

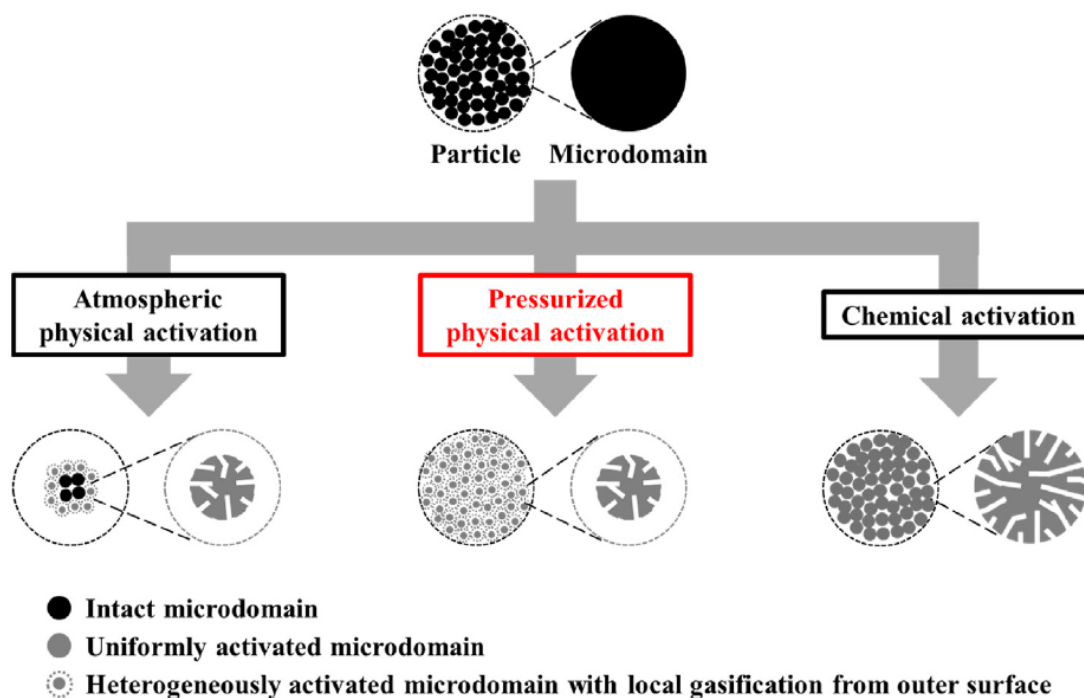


Figure 10. Schematic diagram of differences in atmospheric pressure physical, pressurized physical, and chemical activation processes.⁵⁾ (Reprinted from Carbon, 183, 735–742. Copyright (2021), with permission from Elsevier.)

respectively. Therefore, from the STM results, pressurization was considered not effective to improve a diffusivity of activating gas into microdomains.

A schematic model of the difference in pore development of the atmospheric pressure physical, pressurized physical, and chemical activation methods was proposed based on the microdomain structure model (**Figure 10**). In the case of chemical activation, a sufficient diffusivity of the activating agent in both carbon particles and microdomains allowed uniform reaction of the activating agents with each microdomain in the carbon particle. Therefore, intra-microdomain pores are well developed, giving rise to a high degree of pore development and activation yield for chemical-AC. On the other hand, low diffusivity of activating agent in conventional atmospheric pressure physical activation causes local gasification reactions at the

outer surfaces of carbon particles and microdomains, resulting in low degree of pore development and activation yield. In contrast, observations of particles and microdomains revealed that pressurization improved the activating agent diffusivity in carbon particles, but not in their microdomains. That is, the remarkable increases in SSA and total pore volume for pressurized-AC is very possibly due to the development of not only intra-microdomain pores for most of microdomains consisting of carbon particles, but also inter-microdomain pores. Therefore, the pressurized physical activation method can provide a high degree of pore development, between chemical and atmospheric pressure physical activation methods.

4. Applicability of pressurized physically activated carbon as an adsorbent in adsorption heat pumps⁶⁾

Among various heat pump systems, adsorption heat pump (AHP) has advantages, such as low power consumption, minimal vibration and noise, operable by solar heat or industrial low-temperature waste heat. For the widespread usage, however, a downsizing of AHP devices is required. Existing commercial AHP systems use synthetic zeolite and water as an adsorbent and a refrigerant, respectively. As an alternative promising pair with larger adsorption capacity, AC-ethanol receives attention.^{13–16)} For example, we have reported that slit-shaped carbon micropores of 1.6 nm in width showed the remarkable effective adsorption amount of ethanol under a condition of 10°C/30°C/80°C for cooling water/surrounding environment/regeneration temperatures, respectively.¹⁷⁾

As introduced in Section 3, pressurized-AC showed not only a high degree of pore development, but also a characteristic pore size distribution with a peak for a pore width of approximately 1.6 nm. In this study, therefore, the applicability of pressurized-AC as an adsorbent in AC-ethanol AHP system was examined.

In addition to atmospheric-AC (P0.1T900m90) and pressurized-AC (P1T900m5) shown in Section 2, another AC was prepared by chemical activation method at 900°C using KOH as an activating agent from a spherical carbon (C6). In this section, ACs prepared by atmospheric pressure physical activation, pressurized physical activation, and chemical activation are designated as PAC, PPAC, and CAC, respectively.

Pore size distributions of C6, PAC, PPAC, and CAC are shown in **Figure 11**.

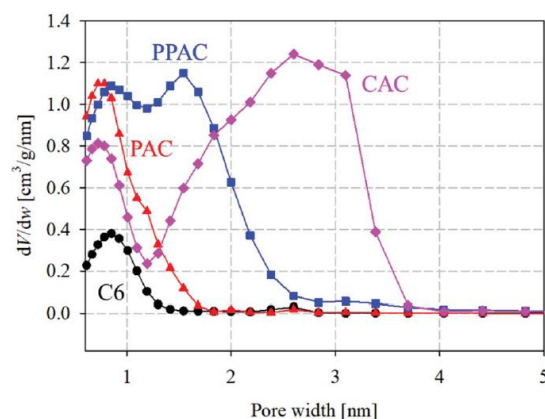


Figure 11. Pore size distributions for starting carbonized material and derived activated carbons. (circle) C6; (triangle) PAC; (square) PPAC; (diamond) CAC.⁶⁾ (Reproduced from Ref. 6 with permission from the Royal Society of Chemistry.)

Conventional atmospheric pressure physical activation using CO₂ as an activating gas predominantly introduced narrow micropores (< 1.0 nm), but CAC prepared by chemical activation using KOH as an activating agent possessed a large amount of mesopores. PPAC showed a bimodal pore size distribution in micropore region.

To assess the applicability in AHP systems with ethanol refrigerant, ethanol adsorption and desorption isotherms were measured at 30°C. Assuming the AHP operation temperatures as 10°C/30°C/80°C for cooling water/surrounding environment/regeneration, a difference of adsorption amounts at 0.1–0.3 of relative pressure (P/P_0) of ethanol adsorption isotherm at 30°C, which is called as effective adsorption amount, is a good index to estimate a performance as AHP adsorbent. Together with the saturated adsorption amounts calculated from a value at $P/P_0 = 0.95$, the effective adsorption amounts of each sample are tabulated in **Table 1**. C6 showed low value of effective adsorption amount (10 mg/g). For PAC, the

Table 1. Saturated and effective ethanol adsorption amounts of starting carbonized material and derived activated carbons.⁶⁾ (Reproduced from Ref. 6 with permission from the Royal Society of Chemistry.)

Sample	Saturated adsorption amount of ethanol [mg/g]	Effective adsorption amount of ethanol	
		On a weight basis [mg/g]	On a volume basis [mg/cm ³]
C6	170	10	8
PAC	730	70	40
PPAC	1730	570	220
CAC	1630	580	120

saturated adsorption amount of ethanol increased remarkably to 730 mg/g as compared with C6 (170 mg/g), whilst an increase of the effective adsorption amount was limited (70 mg/g). This indicates that PAC is not suitable as an adsorbent for the ethanol AHP system, because mainly introduced pores by conventional atmospheric pressure physical activation were narrow micropores. On the other hand, PPAC showed a comparably large effective adsorption amount of ethanol (570 mg/g) with CAC. The characteristic pore size distribution of PPAC having a larger number of optimum pore size of 1.6 nm should provide the high ethanol uptake at $P/P_0 = 0.1-0.3$.

In addition to the effective adsorption amount of a weight basis of adsorbent, the effective adsorption amount per unit volume is important, considering a downsizing of AHP devices. **Figure 12** shows adsorption and desorption isotherms of ethanol at 30°C on an adsorbent volume basis. The effective adsorption amounts of ethanol on a volume basis for C6 and the derived ACs are also shown in **Table 1**. Here, the volume basis adsorption amounts were calculated from the ethanol adsorption amounts on a weight basis and the bulk density (C6: 0.84 g/cm³,

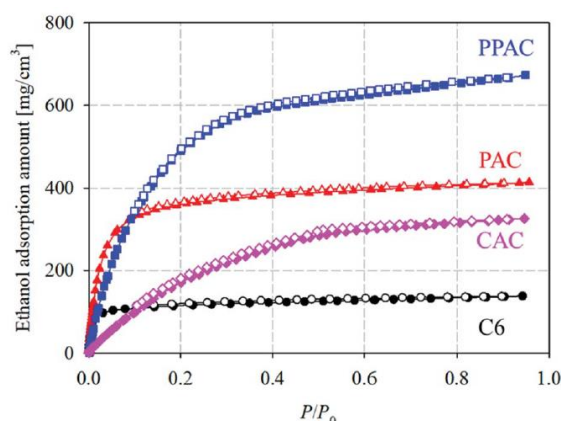


Figure 12. Ethanol adsorption and desorption isotherms on an adsorbent volume basis at 30°C of starting carbonized material, and the derived activated carbons (circle: C6; triangle: PAC; square: PPAC; diamond: CAC).⁶⁾ (Reproduced from Ref. 6 with permission from the Royal Society of Chemistry.)

PAC: 0.57 g/cm³, PPAC: 0.39 g/cm³, CAC: 0.21 g/cm³). Although the effective adsorption amount on a volume basis for CAC remained 120 mg/cm³, PPAC showed a high value of 220 mg/cm³. This is because PPAC possessed “effective” pores for an enlargement of effective adsorption amount of ethanol, but wide pores including mesopores of CAC were less effective.

In summary, it was demonstrated that pressurized physically activated carbon has a great potential as an adsorbent for AHP system with ethanol refrigerant.

5. Conclusion

As well as surface character, porosity governs the performance of porous carbons including activated carbons. In this article, firstly, a difference of pore development mechanisms between physical and chemical activations was introduced based on microdomain structure model. Understanding of the mechanism proposed a novel pressurized physical activation method, and the effectiveness of pressurization on pore development was experimentally confirmed. Finally, a superior volumetric adsorbability of ethanol of the pressurized physically activated carbon was demonstrated as compared with chemically activated carbon, showing the great potential as an adsorbent in adsorption heat pump system using ethanol as a refrigerant.

Demand of high-performance porous carbon materials is growing and growing. In addition to continuous efforts on the improvement of porosity, we are struggling to develop methods to arbitrarily and selectively control the pore size and its distribution and surface characteristic of porous carbon materials.^{18), 19)}

6. Acknowledgements

Special thanks to ASAHI YUKIZAI CORPORATION for providing the spherical phenol resins.

All results shown here were never achieved without great cooperation of my colleagues, especially Prof. Seong-Ho Yoon, Prof. Isao Mochida, Dr. Koji Nakabayashi, Dr. Hyun-Sig Kil, Dr. Doo-Won Kim, and Dr. Hyeonseok Yi. I would like to express my deepest gratitude to you all.

References

- 1) S.-H. Yoon, S. Lim, S.-h. Hong, W. Qiao, D. D. Whitehurst, I. Mochida, B. An, K. Yokogawa, *Carbon*, **2005**, *43*, 1828–1838.
- 2) N. Shiratori, K. J. Lee, J. Miyawaki, S.-H. Hong, I. Mochida, B. An, K. Yokogawa, J. Jang, S.-H. Yoon, *Langmuir*, **2009**, *25*, 7631–7637.
- 3) W. Li, D. Long, J. Miyawaki, W. Qian, L. Ling, I. Mochida, S.-H. Yoon, *J. Mater. Sci.*, **2012**, *47*, 919–928.
- 4) D.-W. Kim, H.-S. Kil, K. Nakabayashi, S.-H. Yoon, J. Miyawaki, *Carbon*, **2017**, *114*, 98–105.
- 5) H. Yi, K. Nakabayashi, S.-H. Yoon, J. Miyawaki, *Carbon*, **2021**, *183*, 735–742.
- 6) H. Yi, K. Nakabayashi, S.-H. Yoon, J. Miyawaki, *RSC Adv.*, **2022**, *12*, 2558–2563.
- 7) H. Marsh, D. Crawford, T. M. O'Grady, A. Wennerberg, *Carbon*, **1982**, *20*, 419–426.
- 8) N. Yoshizawa, K. Maruyama, Y. Yamada, M. Zielinska-Blajet, *Fuel*, **2000**, *79*, 1461–1466.
- 9) N. Yoshizawa, K. Maruyama, Y. Yamada, E. Ishikawa, M. Kobayashi, Y. Toda, M. Shiraishi, *Fuel*, **2002**, *81*, 1717–1722.
- 10) H. Marsh, D. S. Yan, T. M. O'Grady, A. Wennerberg, *Carbon*, **1984**, *22*, 603–611.
- 11) H. Shimanoe, S. Ko, Y.-P. Jeon, K. Nakabayashi, J. Miyawaki, S.-H. Yoon, *Polymers*, **2019**, *11*, 1911–1925.
- 12) J. Miyawaki, *Tanso Zairyo no Kenkyu Kaihatsu Doko 2022 (CPC Society annual report)*, **2022**, *CPC Society*, pp. 158–179 (in Japanese).
- 13) I. I. El-Sharkawy, K. Uddin, T. Miyazaki, B. B. Saha, S. Koyama, J. Miyawaki, S.-H. Yoon, *Int. J. Heat Mass Transfer*, **2014**, *73*, 445–455.
- 14) K. Uddin, I. I. El-Sharkawy, T. Miyazaki, B. B. Saha, S. Koyama, H.-S. Kil, J. Miyawaki,

- S.-H. Yoon, *Appl. Therm. Eng.*, **2014**, *72*, 211–219.
- 15) A. Pal, K. Thu, S. Mitra, I. I. El-Sharkawy, B. B. Saha, H.-S. Kil, S.-H. Yoon, J. Miyawaki, *Int. J. Heat Mass Transfer*, **2017**, *110*, 7–19.
- 16) P. Huo, Y. Zhang, L. Zhang, M. Yang, W. Wei, X. Zhang, J. Yang, Y. Zhang, *Ind. Eng. Chem. Res.*, **2021**, *60*, 11141–11150.
- 17) T. Miyazaki, J. Miyawaki, T. Ohba, S.-H. Yoon, B. B. Saha, S. Koyama, *AIP Conf. Proc.*, **2017**, *1788*, 020002.
- 18) Y. Yu, H.-S. Kil, K. Nakabayashi, S.-H. Yoon, J. Miyawaki, *AIP Conf. Proc.*, **2019**, *2097*, 02002.
- 19) Y. Yu, J. Miyawaki, *Carbon*, **2020**, *170*, 380–383.